

See discussions, stats, and author profiles for this publication at: <https://www.researchgate.net/publication/26818340>

# Synthesis and Photophysics of Core-Substituted Naphthalene Diimides: Fluorophores for Single Molecule Applications

ARTICLE *in* CHEMISTRY - AN ASIAN JOURNAL · SEPTEMBER 2009

Impact Factor: 4.59 · DOI: 10.1002/asia.200900215 · Source: PubMed

CITATIONS

34

READS

136

8 AUTHORS, INCLUDING:



**Chintan Jani**

Monash University (Australia)

8 PUBLICATIONS 389 CITATIONS

SEE PROFILE



**Sheshanath V Bhosale**

RMIT University

129 PUBLICATIONS 2,488 CITATIONS

SEE PROFILE



**Frans C De Schryver**

University of Leuven

670 PUBLICATIONS 21,277 CITATIONS

SEE PROFILE



**Steven J Langford**

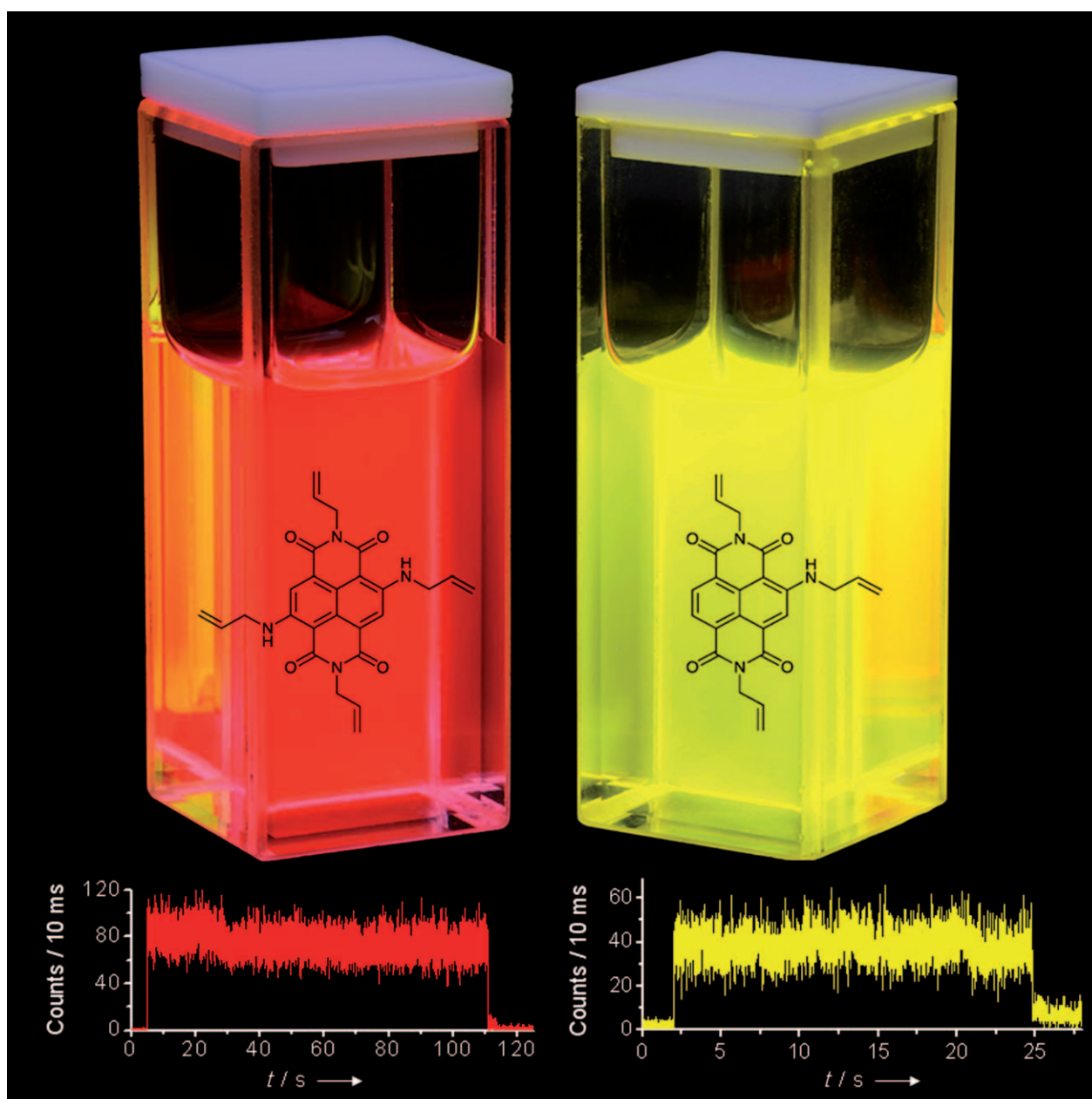
Monash University (Australia)

146 PUBLICATIONS 3,331 CITATIONS

SEE PROFILE

# Synthesis and Photophysics of Core-Substituted Naphthalene Diimides: Fluorophores for Single Molecule Applications

Toby D. M. Bell,<sup>\*,[a]</sup> Sheryll Yap,<sup>[a]</sup> Chintan H. Jani,<sup>[b]</sup> Sheshanath V. Bhosale,<sup>[b]</sup> Johan Hofkens,<sup>[c]</sup> Frans C. De Schryver,<sup>[c]</sup> Steven J. Langford,<sup>\*,[b]</sup> and Kenneth P. Ghiggino<sup>\*,[a]</sup>



**Abstract:** The synthesis and photophysics of two new aminopropenyl naphthalene diimide (SANDI) dyes are reported. A general and convenient method for the synthesis of the precursor mono-, di-, and tetrabrominated 1,4,5,8-naphthalene tetracarboxylic dianhydrides is described. The two core-substituted SANDIs exhibit many of the photophysical properties required for fluorescence labeling applications including high photostability and high fluorescence quantum yields ( $>0.5$ ) in the visible region of the spectrum. The

emission wavelength is sensitive to the number of substituents on the NDI core, and the fluorescence decay times are in the range of  $\sim 8$ – $12$  ns for both compounds in the solvents investigated. Preliminary fluorescence emission data from single molecules of the compounds embedded in poly(methyl

**Keywords:** core-substitution • energy transfer • fluorescence • naphthalene diimide • single molecule fluorescence

methacrylate) films are also reported and show that single molecules have very low yields of photobleaching, particularly the di-substituted system. Furthermore, only a small proportion ( $<10\%$ ) of the single molecules studied display fluorescence intermittencies or “blinks” in their photon trajectory. The compounds appear to be excellent candidates for applications at the single molecule level, for example, as FRET labels.

## Introduction

There has been a rapid expansion in the use of single molecule (SM) fluorescence techniques to address questions in an increasing range of research areas, particularly in biophysics.<sup>[1–3]</sup> The attraction of SM studies is that information regarding individual molecules is not lost arising from ensemble-averaging, thus providing a detailed understanding of the underlying distribution of behaviors that contribute to the bulk sample properties.

Many spectroscopic and microscopic techniques for studying molecular properties and dynamics are based on detecting luminescence from the substrate. One approach to studying materials which are not intrinsically fluorescent is to attach a suitable fluorescent moiety to the substrate of interest. Such fluorescent labels or “tags” offer the sensitivity and environment-based modulation effects (e.g., in response


to pH or polarity), required for reporting on the behavior of the substrate. There is an increasing need for new and improved fluorophores capable of meeting the demands of the ever-widening range of applications, particularly at the molecular level where many labels routinely used in ensemble measurements are not suitable. Characteristics of a good fluorescence label include a large absorption cross-section (molar absorption coefficient,  $\epsilon_r$ ) and high fluorescence quantum yield, ( $\Phi_f$ ) in the visible or near IR spectral regions for easy detection at low labeling levels. Fluorescence labels for SM applications also need to be highly photostable and thus able to withstand multiple emission/excitation cycles. Ideally, at least  $10^6$  photons (cycles) should be emitted prior to irreversible photobleaching of the molecule. Relatively long fluorescence lifetimes (on the nanosecond scale) are another useful property for SM labels to enable the dynamics of processes in this time regime to be monitored. Fluorescence intermittencies, or “blinking” arising from excursions to non-fluorescent states or reversible quenching processes, is considered an undesirable trait for fluorophores used as SM labels. However, a favorable characteristic of fluorophores is sensitivity of the emission spectrum to changes in molecular structure of the core chromophore. Thus, by altering substituents one can effectively tune the emission of a molecule to accommodate various applications such as suitability for fluorescence energy transfer experiments.

Examples of compounds that fulfill these requirements and are currently used as fluorescence labels include laser dyes such as rhodamines, cyanines, oxazines, and imide derivatives of rigid polynuclear aromatic hydrocarbons, such as perylene. The latter class have proven particularly suited to

[a] Dr. T. D. M. Bell, S. Yap, Prof. K. P. Ghiggino  
School of Chemistry and Bio21 Institute  
The University of Melbourne  
Parkville, Victoria, 3010 (Australia)  
Fax: (+61)3-9348-1595  
E-mail: tbell@unimelb.edu.au

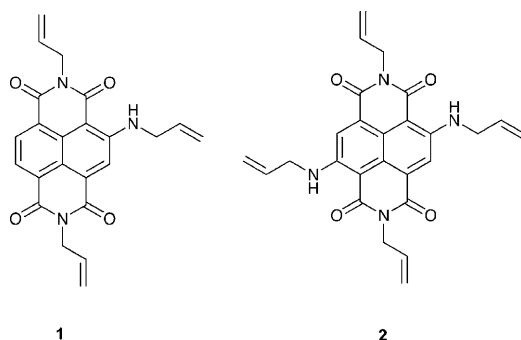
[b] C. H. Jani, Dr. S. V. Bhosale, Prof. S. J. Langford  
School of Chemistry  
Monash University  
Clayton, Victoria, 3800 (Australia)

[c] Prof. J. Hofkens, Prof. F. C. De Schryver  
Department of Chemistry  
Katholieke Universiteit Leuven  
200F Celestijnenlaan, 3001 Heverlee (Belgium)

 Supporting information for this article is available on the WWW under <http://dx.doi.org/10.1002/asia.200900215>.

SM spectroscopy owing to their high fluorescence quantum yields (often >0.9) and photostability.<sup>[4,5]</sup> Unlike the larger imide substituted rylene dyes (perylene, terylene, and quaterylene), unsubstituted naphthalene diimides (NDIs) have low  $\Phi_f$  values and emission is usually confined to the UV region of the spectrum,<sup>[6,7]</sup> making them unsuitable as fluorescence labels. The introduction of amino substituents, however, to the *ortho* position of the imide functionality results in their transformation into colored, highly fluorescent dyes<sup>[8–12]</sup> and makes them potentially useful fluorescence label candidates. It is with this versatility in properties that NDIs have found popularity in the latter half of the 20<sup>th</sup> century<sup>[13]</sup> arising, in part, from the pioneering work of Vollmann in the early 1930s.<sup>[14]</sup>

The realization that NDIs can act as useful components for the creation of supramolecular functional materials<sup>[13,15–17]</sup> has transpired as a result of their desirable electronic and spectroscopic properties over pyromellitic diimides. Their enhanced solubility properties over perylene diimide dyes also can assist synthetic manipulation and expands the range of potential applications. Vollmann's synthesis of 2,6-diarylamino core-substituted NDIs from 2,6-dichloro-1,4,5,8-naphthalenetetracarboxylic dianhydride which itself was derived in four steps from pyrene, is still used as a source of precursors.<sup>[13]</sup> His description of their fluorescent properties as dull and non-fluorescent,<sup>[14]</sup> may well be the reason why this class of core-substituted NDIs have not received much attention until recently.<sup>[8–12,13,16]</sup> Herein, we report on the synthesis and photophysical characterization of two new substituted aminopropenyl naphthalene diimide (SANDI) derivatives **1** and **2** (Scheme 1) which show potential as functionalizable fluorescence labels which absorb and emit in the visible part of the spectrum.



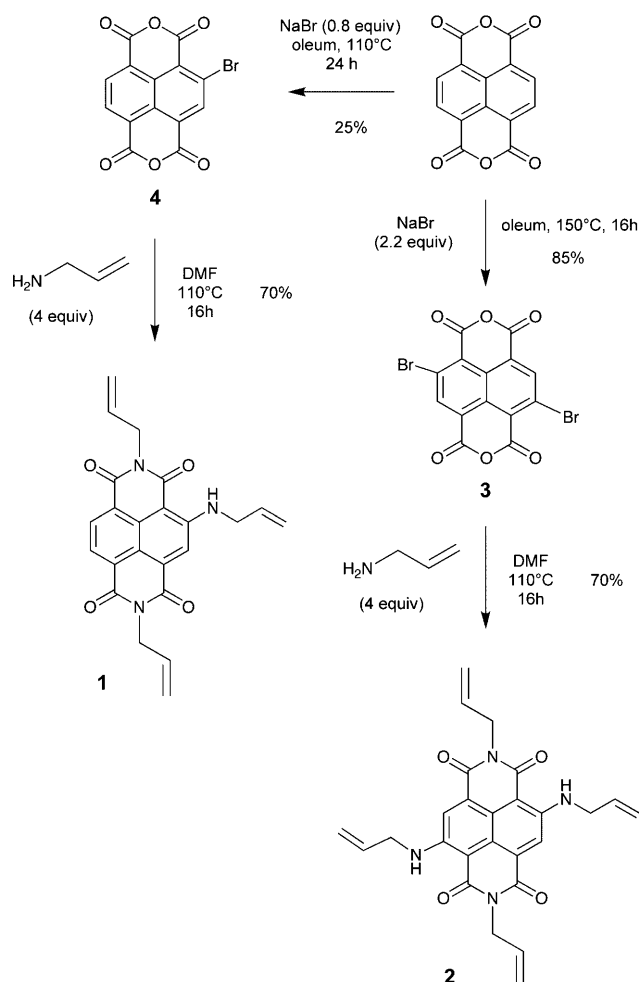
Scheme 1. Molecular structures of mono-allyl SANDI **1** and di-allyl SANDI **2** used in this work. The terms mono- and di-allyl refer to core substitution only.

We also report some preliminary SM data which indicate that these molecules are sufficiently bright and photostable to meet the exacting requirements of many SM experimental applications. Of particular note, is the low occurrence of fluorescence blinking observed from SMs of **1** and, especially, **2** when embedded in poly(methyl methacrylate) (PMMA) films. The presence of the propenyl functionality

in the molecules imparts further possibilities for synthetic modification (including polymer formation) and increases their potential for use in new applications.

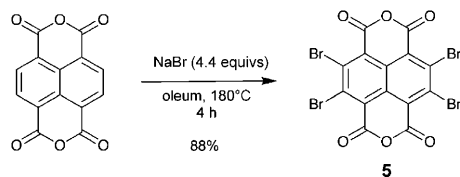
## Results and Discussion

Compounds **1** and **2** were prepared in good yield by the reaction of allylamine with 2-bromo- and 2,6-dibromo-1,4,5,8-naphthalenetetracarboxylic dianhydride (NDA), respectively, following literature procedures (Scheme 2).<sup>[8]</sup> The importance of the per-halogenated core substituted NDAs such as **3** and **4**, has recently lead to two reported syntheses involving molecular bromine<sup>[18]</sup> or dibromoisocyanuric acid (DBI)<sup>[9,19]</sup> in oleum as the brominating agent. In our hands, as in others,<sup>[9]</sup> the reaction involving molecular bromine could not be reproduced in high yield and DBI is not readily available in large quantity. We have recently discovered that halogenation can be easily achieved using sodium bromide in oleum (Scheme 2) and that pathways to the 2-bromo **4**, 2,6-dibromo **3**, and 2,3,6,7-tetrabromo-1,4,5,8-naphthalene



Scheme 2. The NaBr method leads to highly core-functionalized naphthalene diimides in high yield from cheap and readily available starting materials.

tetracarboxylic acid dianhydrides **5** (Scheme 3) are achievable by varying the reaction conditions (temperature, time, concentration) and stoichiometry of NaBr used.



Scheme 3. The NaBr method leads to the tetrabromo derivative in high yield on multi-gram scale.

Reaction of NaBr (0.8 equivalents) with 1,4,5,8-naphthalenetetracarboxylic dianhydride in oleum (20% free SO<sub>3</sub>) for 24 h at 110°C leads to the formation of the monobromo NDA **4** in a moderate 25% yield (Scheme 2). The reaction conditions reflect a compromise between actual yield and ease of separation from starting dianhydride or the dibromo NDA by-product **3** which occurs on further exposure to NaBr or at higher temperature. Reaction of **4** with allylamine in DMF at elevated temperature yields the diimide **1** in 70% yield after chromatography. Increasing the amount of NaBr (2.2 equivalents) under similar conditions leads to the clean formation of the dibromo NDA **3** as the major product.<sup>[20]</sup> Reaction of **3** with allylamine in DMF yields the diimide **2** in 70% yield after chromatography. It is worth noting that a core trisubstituted NDI has been recently prepared from the corresponding dichloro-NDI using a 1,2-diamine,<sup>[10]</sup> however, none of this type of product was seen under the conditions employed here. The efficiency of the reaction to form the dibromo derivative manifests itself from the reduced reactivity associated with further bromination. More forcing conditions and higher stoichiometry of NaBr (4.4 equiv) does lead to the tetrabromo-NDA **5** in 88% yield (Scheme 3).<sup>[21]</sup> Hence by this method, a range of core-substituted NDAs are possible.

Crystals of **5** suitable for X-ray crystallography were grown by vapor diffusion of water into a DMSO solution of **5**.<sup>[22]</sup> The crystal structure (Figure 1) shows a twisted aromatic core, which is unusual compared to other NDI structures.<sup>[6,23,24]</sup> The twist is imparted by the steric bulk of the *ortho* bromines.

The torsion of the bromine atoms and the oxygen atoms can be calculated as deviation from the mean plane of the naphthalene ring in the molecule.<sup>[25]</sup> While Br(1) (Figure 1a) sits in plane with the naphthalene core (deviation: 0.1 Å), Br(2) is out of the plane by 2.1 Å. The carbonyl oxygens adjacent to the bromines that twist out of the plane (O(3)) are themselves out of the plane by 2.05 Å arising from steric strain. Furthermore, the anhydride oxygens are twisted out of the plane substantially with a deviation of 4.6 Å. The molecules exhibit  $\pi$ -stacking interactions in the crystal lattice (Figure 1b), with intermolecular separations of 3.5 Å between aromatic planes within the NDA, leading to channels filled by ordered DMSO solvent molecules.

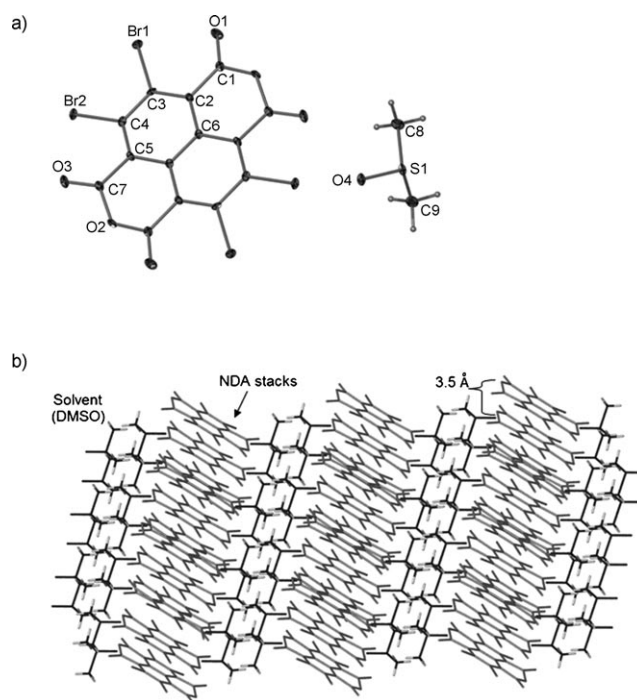


Figure 1. a) Crystal structure of 2,3,6,7-tetrabromo-1,4,5,8-naphthalenetetracarboxylic dianhydride **5** from DMSO solvent. b) A representation of a portion of the crystal lattice of **5**.DMSO. NDA=naphthalene dianhydride.

### Ensemble Photophysical Properties of **1** and **2**

Figure 2 shows the steady-state absorption and emission spectra of both **1** (upper panel) and **2** (lower panel) in toluene, ethanol, and acetonitrile. The absorption maxima in the near-UV spectral region are typical of unsubstituted NDIs and for such systems, this is the lowest energy transition

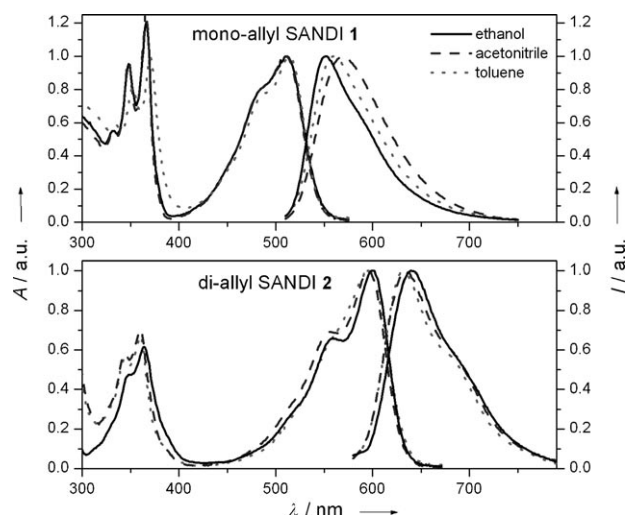


Figure 2. Normalized steady state absorption and corrected emission spectra of **1** (panel a) and **2** (panel b) in toluene (light grey, dot), acetonitrile (grey, dash), and ethanol (black, line).  $\lambda_{\text{ex}}$  = 450 and 500 nm, for emission spectra of **1** and **2**, respectively.



(S<sub>0</sub>–S<sub>1</sub>). For compounds **1** and **2**, however, a new, additional, lower energy transition is present in the visible region of their absorption spectra with maxima in toluene at 513 and 601 nm, respectively. Similar transitions have also been observed in other NDI compounds with electron donating side groups.<sup>[8,9]</sup> This new transition is polarized in the opposite direction (along the short axis) to the near-UV transition which is polarized along the long axis of the molecules and remains mostly unaffected with respect to unsubstituted NDI. Calculations by Würthner and co-workers<sup>[8]</sup> on related SANDI compounds also showing a similar new transition indicate that it has some charge transfer character. The strength of the new transition is assisted by intramolecular hydrogen bonding between the H atom attached to the amino N atom and the nearby carbonyl O atom. This hydrogen bond then forms part of a 6-membered ring and helps confer planar geometry on the atoms involved. Maximal overlap of the lone pair on the N atom with the conjugated pi-system of the core is realized when the dihedral angle of the core–N bond is planar (0° or 180°).

It can be readily seen in Figure 2 how the addition of the second alkylamino substituent leads to a red shift in the absorption and emission maxima, highlighting the spectral tunability of these compounds by means of the number and placement of the substituents. On the other hand, only small spectral shifts are observed with changes of solvent. The emission maximum of **1** red shifts only 8 nm (260 cm<sup>−1</sup>) from 551 nm in toluene to 559 nm in acetonitrile and a further 11 nm (345 cm<sup>−1</sup>) to 570 nm in ethanol. The emission maximum of **2** is at 632 nm in toluene, 634 nm in acetonitrile, and 638 nm in ethanol (a total of 150 cm<sup>−1</sup> red shift compared to 605 cm<sup>−1</sup> for **1**). It is likely that the increased symmetry of **2** balances the charge redistribution with respect to **1** leading to the weaker solvent dependent red shift observed. Similar, although more pronounced, solvatochromic behavior was seen for the SANDI compounds of Würthner.<sup>[8,9]</sup>

Compounds **1** and **2** were found to have values for  $\epsilon_r$  in toluene of 11000 M<sup>−1</sup> cm<sup>−1</sup> and 13100 M<sup>−1</sup> cm<sup>−1</sup>, respectively. These values lie at the lower end of the range generally exhibited by fluorescent labels and are similar to those reported for related SANDI compounds.<sup>[8,9]</sup> Both SANDI derivatives display favorably high fluorescence efficiencies in all three solvents, with  $\Phi_f$  values typically > 0.5 (Table 1). Fluorescence decay profiles were also recorded in toluene, ethanol, and acetonitrile using the time correlated single photon counting method and fluorescence decay times ( $\tau_{flu}$ ) were obtained by fitting the decay profiles with an exponential

decay function convolved with an instrument response function using a least squares fitting routine based on the Marquardt algorithm. Satisfactory fits to the data (assessed by the reduced  $\chi^2$  goodness-of-fit parameter and a random distribution of the weighted residuals) were obtained for both SANDI compounds in all solvents. Fluorescence decay times followed the same trend for both SANDIs: the longest decay time for each compound was recorded in acetonitrile, the shortest in ethanol and decay times are longer for **2** than for **1** in all solvents (Table 1).

The fluorescence lifetimes of both compounds are relatively long: for **1**  $\sim 8 < \tau_{flu} < 11$  ns and **2**  $\sim 9 < \tau_{flu} < 12$  ns with some dependence on solvent. These values compare favorably to those of most commonly used dyes, including perylene and terrylene imides. Longer lifetimes are desirable for a number of reasons, the primary advantages being ease of detection and greater confidence in the interpretation of small differences owing to changes in experimental conditions.

As a result of their relatively long fluorescence decays and spectral characteristics, **1** and **2** are well suited for use as labels in Förster resonant energy transfer (FRET) applications. The critical distance,  $R_o$ , for through space energy transfer is defined as the separation of the donor and acceptor at which energy transfer occurs with 50% efficiency and is given by Equation (1),

$$R_o = 0.2108(\eta^4 \Phi_f \kappa^2 J)^{1/6} \quad (1)$$

where,  $\eta$  is the refractive index of the medium,  $\Phi_f$  the fluorescence quantum yield of the donor in the absence of the acceptor,  $\kappa^2$  the orientation factor for the dipole–dipole interaction, and  $J$  is the normalized spectral overlap integral. Assuming a value of 2/3 for  $\kappa^2$  (for a random orientation of the donor and acceptor transition dipoles), the critical Förster distance for the mono-allyl and di-allyl pair is 41 Å implying that FRET processes should be readily observable for donor–acceptor separations in the 2–7 nm range.

### Single Molecule Photophysical Properties of **1** and **2**

Single molecules of both the SANDI compounds are bright and readily imaged by confocal fluorescence microscopy. Some example fluorescence trajectories of single molecules of **1** and **2** embedded in PMMA films and studied under nitrogen are shown in Figures 3 and 4, respectively. Single molecules of both SANDIs emit with high count rates typically in the range of  $(5\text{--}10) \times 10^3$  counts/second under the experimental conditions employed. As a comparison, perylene monoimide under similar conditions displayed count rates about 2–3 times higher.<sup>[4]</sup>

Trajectories of **1** typically lasted of the order of some sec-

Table 1. Selected ensemble photophysical data for **1** and **2** in various solvents.

SANDI	Solvent	$\lambda_{\text{max(abs)}} [\text{nm}]$	$\epsilon_r [\text{M}^{-1} \text{cm}^{-1}]$	$\lambda_{\text{max(em)}} [\text{nm}]$	$\Phi_f$	$\tau_{flu} [\text{ns}]$
<b>1</b>	toluene	513	11 000	551	0.51	9.5
<b>1</b>	EtOH	511	–	570	0.44	7.7
<b>1</b>	MeCN	511	–	559	0.65	11.2
<b>2</b>	toluene	601	13 100	632	0.62	11.3
<b>2</b>	EtOH	596	–	638	0.60	9.5
<b>2</b>	MeCN	595	–	634	0.56	11.8

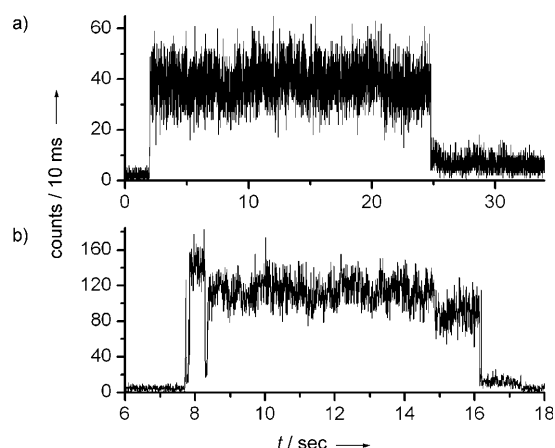


Figure 3. Emission intensity trajectories as a function of time for two single molecules (panels a and b) of **1** in PMMA film under nitrogen. Excitation was at 485 nm.

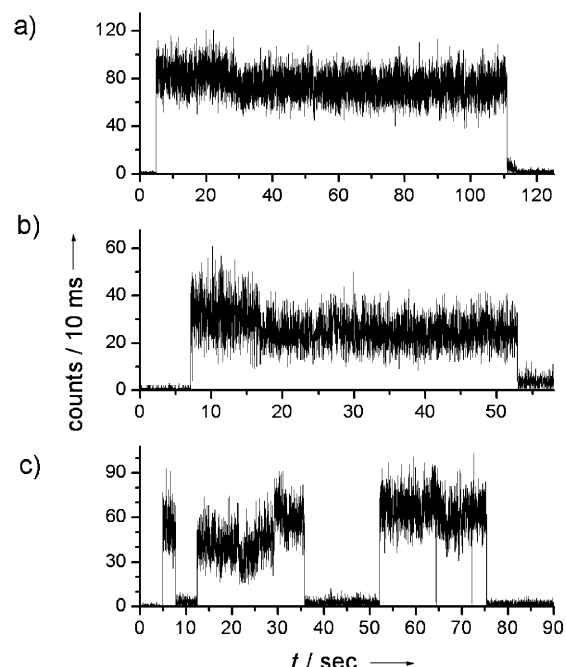


Figure 4. Emission intensity trajectories as a function of time for 3 single molecules (panels a, b, and c) of **2** in PMMA film under nitrogen. Excitation was at 543 nm.

onds before photobleaching occurred. The trajectory shown in Figure 3a was the longest lived of the data set at 23 s, while the trajectory in Figure 3b lasting for 8 s is typical of SMs of **1**. Di-allyl SANDI **2**, however, shows much greater photostability with some single molecules emitting for over a minute such as the SM in Figure 4a. Also apparent in the photon trajectories is the almost complete lack of interruptions to the fluorescence emission or “blinking”. Visits to the triplet state are the most prevalent blinking mechanism and occur on a micro to millisecond time range for most fluorophores. Excessive triplet formation can severely restrict

the application of a fluorophore as a SM label as the molecules will be ‘off’ for considerable periods. These SM measurements were carried out under a nitrogen atmosphere and even when the data are binned in short 1 ms intervals, there are no obvious triplet blinks implying that these compounds have a very low yield of triplet formation. Fluorescence interruptions on a timescale of 100s of ms to seconds, associated with reversible quenching processes, are also often observed in many single molecule fluorescence studies and can be a severe hindrance to emitter performance. Long blinks such as those in the trajectory of the SM in Figure 4c were seen in approximately a third of the trajectories recorded from SMs of **1** and in less than 10% of the trajectories of SMs of **2**. Fluctuations in emission intensity, such as are evident in the trajectory of **1** shown in Figure 3b, were almost entirely absent for SMs of **2**. Indeed, most SMs of **2** showed steady, single level emission with no intermittencies before photobleaching in one step—essentially ideal fluorophore behavior for SM labeling applications.

Example emission spectra from a single molecule of **2** in PMMA film under nitrogen are shown in Figure 5. Successive spectra were taken every three seconds thus providing a

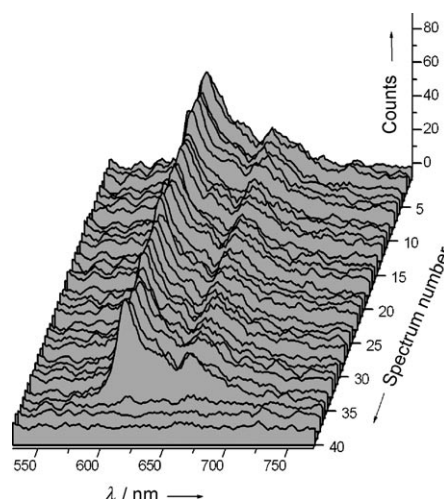


Figure 5. Emission spectra from a single molecule of **2** embedded in a PMMA film under nitrogen. Successive spectra are recorded every three seconds. Excitation was at 543 nm.

record of changes in the emission with time. Most molecules showed very stable emission in terms of spectral characteristics which resemble well the spectra of bulk solutions. Very little spectral shifting over time was observed for individual molecules. Most molecules behaved similarly to the one in Figure 5 showing a constant wavelength of emission maximum throughout their trajectory. Emission maxima varied somewhat from molecule to molecule and were distributed over the range of 580–650 nm, reflecting local heterogeneities in the PMMA film. The small difference in average SM emission maximum (~615 nm) and the ensemble values (~630 nm) is attributed to differences between the film and solution environments.

The two SANDI molecules synthesized and studied here show many properties desirable for fluorescence labeling applications. They have high emission quantum yields ( $>0.5$ ), absorption and emission in the visible part of the spectrum, and nanosecond fluorescence decay times. Most importantly, they also show excellent photostability. Aerated solutions ( $\sim 10^{-5}$  M) of **1** and **2** in toluene were subjected to eight hours of irradiation from the focused output of a 150 W Xe arc lamp. Over this time, **1** underwent photobleaching of only  $\sim 6\%$  while **2** showed no observable change in absorption during irradiation. From the known spectral intensity of the lamp, this indicates a yield of photobleaching of the order of  $10^{-6}$  for **1** and less than  $10^{-7}$  for the di-allyl compound **2**.

This very low photobleaching yield is realized at the SM level for **2** with some molecules undergoing tens of millions of cycles of excitation and photon emission before photobleaching. For example, approximately 800,000 photons from the single molecule shown in Figure 4a were detected by the APD detector before the molecule photobleached. Taking into account that the total detection efficiency of the experimental set-up is only about 5% and that half of the collected photons were directed to the CCD camera, the actual number of photons that this one single molecule emitted is of the order of 30 million. The longest lived single molecule of **2** emitted a steady stream of  $\sim 4500$  photons per second for longer than 10 min, implying that more than 100 million cycles of excitation and emission were achieved before photobleaching occurred.

Although these preliminary SM data sets are small ( $<50$  molecules) a large variation in emission intensity (count rate) from molecule to molecule is noted. Not nearly so much variation in count rate over time (aside from “off times”) is observed for single molecules. One possible mechanism that could lead to extensive variation in emission (count rate) is rotation of the alkylamino side arms. Calculations by Würthner and co-workers<sup>[8]</sup> of similar SANDI compounds showed that the alkylamino side group can donate electron density from the lone pair on the nitrogen atom into the naphthalene core as a result of restricted rotation through hydrogen bonding. Electron donation into the core would strengthen the  $S_0$ – $S_1$  transition resulting in an increased rate of photon absorption and, hence, emission (count rate).

The extent of electron donation will be strongly dependent on the angle between the naphthalene core and the alkylamino side arm with electron donation expected to be maximal when the core and side arm are in a planar conformation as this maximizes orbital overlap between the pi-electrons of the core and the nitrogen lone pair. The single bond linking each side arm to the core would be expected to allow the side arms a certain degree of relatively facile rotation. In bulk solution, the equilibrium arrangement would dominate, however, it is quite possible that single molecules embedded in a polymer film could adopt a range of conformations—particularly in a film prepared by rapid spin-casting. Depending on the extent of sensitivity of elec-

tron donation to the substituent side-arm orientation, a range of conformations could lead to a distribution of photophysical behavior. A more detailed study of the photophysics of these new SANDI compounds as single molecules is currently in progress and will be reported subsequently.

## Conclusions

We have developed a convenient, efficient, and scalable alternate reaction protocol for the synthesis of mono-, di-, and tetra-brominated core substituted naphthalenetetracarboxylic dianhydrides. This method will allow easy access to core-substituted NDIs and hence allow further functionalization of these molecules which will have an impact on their fluorescent properties for supramolecular and material chemistry applications. Studies in these areas, and in particular the chemistry of **5**, are underway.

The photophysical properties of two new aminopropenyl substituted derivatives of naphthalene diimide have been characterized in bulk solution in a range of solvents and have undergone preliminary assessment at the single molecule level. Both mono-allyl and di-allyl SANDI compounds show many properties desirable for fluorescence labeling applications such as absorption and emission in the visible part of the spectrum, quantum yields greater than 0.5, nanosecond fluorescence decay times, and a high degree of photostability. The absorption and emission properties are also highly tunable with the addition of the second aminopropenyl group leading to a considerable red-shifting of the emission. The critical Förster distance for a randomly oriented mono-allyl SANDI di-allyl SANDI pair is 4.1 nm suggesting their suitability as FRET labels capable of reporting on separations in the 2–7 nm range. Single molecules of these compounds in PMMA film under nitrogen show strong emission with very few interruptions or “blinks” and good photostability. This is particularly so for the di-substituted compound with some single molecules emitting tens of millions of photons before photobleaching.

## Experimental Section

### Synthetic Procedures

General bromination: Naphthalenetetracarboxylic dianhydride (0.1 mm) in the presence of oleum (20% free  $\text{SO}_3$ , 15 mL) and NaBr is stirred and heated in a Carrius tube for 16–24 h. Slow addition of propionic acid (CAUTION: highly exothermic) precipitates the product as a yellow solid. For **5**: 5 g NDA yields 6.7 g, 62%.

Characterization data for **3**: m.p.:  $>350^\circ\text{C}$ ;  $^1\text{H NMR}$  (400 MHz, DMSO):  $\delta=8.74$  ppm (s, 2H, ArH); mass spectrum (ESI)  $m/z$ : 426  $[M]^-$ . For **4**: m.p.:  $>350^\circ\text{C}$ ;  $^1\text{H NMR}$  (400 MHz, DMSO):  $\delta=8.73$  (d,  $J=4.1$  Hz, 2H, ArH), 8.68 (s, 1H, ArH), 8.67 ppm (d,  $J=4.1$  Hz, 2H, ArH); mass spectrum (ESI)  $m/z$ : 347  $[M+H]^+$ . For **5**: m.p.:  $>350^\circ\text{C}$ ; IR (nujol):  $\tilde{\nu}=1787$ , 1731, 1192, 1174, 1149, 1093, 986, 936  $\text{cm}^{-1}$ ; UV/Vis (DMF):  $\lambda_{\text{max}}=269$ , 363(sh), 377 nm; mass spectrum (ESI)  $m/z$ : 583.55  $[M]^-$ .

General imidation: Compound **4** (100 mg) and allyl amine (4.4 equiv) were stirred in DMF (20 mL) at  $110^\circ\text{C}$  overnight. The reaction mixture was allowed to cool down to room temperature and water (30 mL) was



added. The resulting highly colored precipitate was filtered and collected at the pump, dried in a dessicator, and purified using column chromatography (20% hexane in DCM). Yield of **1** = 70%; m.p.: 195–196°C;  $^1\text{H}$  NMR (300 MHz,  $\text{CDCl}_3$ , see Figure S1 in the Supporting Information):  $\delta$  = 10.23 (brt, 1H, NH), 8.66 (d,  $J$  = 7.8 Hz, 1H, ArH), 8.36 (d,  $J$  = 7.8, 1H, ArH), 8.1 (s, 1H, ArH), 5.9–6.1 (m, 3H, allyl H), 5.1–5.4 (m, 6H, allyl H), 4.83 (dt,  $J$  = 5.8, 1.4 Hz, 2H,  $\text{CH}_2$ ), 4.77 (dt,  $J$  = 5.8, 1.4 Hz, 2H,  $\text{CH}_2$ ), 4.23 ppm (m, 2H,  $\text{CH}_2$ );  $^{13}\text{C}$  NMR (100 MHz,  $\text{CDCl}_3$ , see Figure S2 in the Supporting Information):  $\delta$  = 166.0, 163.1, 162.8, 162.7, 152.5, 132.7, 132.2, 131.7, 131.6, 131.2, 129.6, 127.9, 126.2, 124.9, 123.7, 120.2, 119.6, 118.5, 118.0, 117.7, 45.5, 43.0, 42.5 ppm; MS (MALDI-TOF): 402.1 (100%), ( $\text{M} + \text{H}$ ) $^+$ ; UV/Vis (tol):  $\lambda_{\text{max}}$  ( $\epsilon$ ) = 350, 368, 515 nm (11000); Fluorescence (tol):  $\lambda_{\text{max}}$  = 551 nm. Yield of **2** is 70%; m.p.: 223–224°C;  $^1\text{H}$  NMR (300 MHz,  $\text{CDCl}_3$ , see Figure S3 in the Supporting Information):  $\delta$  = 9.5 (brt, 1H, NH), 8.16 (s, 2H, ArH), 5.9–6.1 (m, 4H, allyl H), 5.1–5.5 (m, 8H, allyl H), 4.81 (dt,  $J$  = 5.5, 1.3 Hz, 4H,  $\text{CH}_2$ ), 4.1–4.2 ppm (m, 4H,  $\text{CH}_2$ );  $^{13}\text{C}$  NMR (100,  $\text{CDCl}_3$ , see Figure S4 in the Supporting Information):  $\delta$  = 165.8, 149.1, 133.4, 132.1, 125.7, 121.2, 118.6, 117.8, 117.6, 117.3, 102.0, 45.4, 42.4, 29.7 ppm; MS (MALDI-TOF): 456.1 (100%), [ $\text{M}$ ] $^+$ ; UV/Vis (tol):  $\lambda_{\text{max}}$  ( $\epsilon$ ) = 346, 362, 602 nm (13100); Fluorescence (tol):  $\lambda_{\text{max}}$  = 629 nm.

#### Single Crystal X-ray Diffraction Experiment

Single crystals of **5** were grown by vapor diffusion of water into a DMSO solution of **5**. X-ray diffraction data was collected on a Nonius Kappa CCD diffractometer (graphite-monochromated  $\text{MoK}_\alpha$  radiation,  $\lambda$  = 0.71073 Å). Structures were solved by direct methods (SHELXS-97) and refined by full-matrix least-squares calculations on  $F^2$  with the SHELXL-TL program package. Non-hydrogen atoms were refined anisotropically. CCDC 649279, contains the supplementary crystallographic data for this paper. These data can be obtained free of charge from The Cambridge Crystallographic Data Centre at [www.ccdc.cam.ac.uk/data\\_request/cif](http://www.ccdc.cam.ac.uk/data_request/cif)

#### Photophysical Measurements

Absorption spectra were recorded using a Varian Cary 50 spectrophotometer and fluorescence spectra were measured using a Varian Cary Eclipse fluorescence spectrophotometer. Fluorescence spectra were corrected for differences in detection efficiency with emission wavelength. All ensemble samples were prepared using spectrophotometric grade solvents used as received from Aldrich and degassed using successive freeze-pump-thaw cycles. Fluorescence decay profiles were recorded using the time-correlated single photon counting technique as outlined elsewhere.<sup>[26]</sup> The excitation source was an optical parametric oscillator (OPO, Coherent) which provided ~100 fs FWHM pulses at 100 kHz. The OPO was pumped by a regeneratively amplified mode-locked Ti:sapphire laser (Coherent Mira). Compounds **1** and **2** were excited at 510 nm and 590 nm, respectively. Emission from the sample was passed through a polarizer oriented at 54.7° relative to the vertically polarized excitation light thereby removing any anisotropic effects from the decay. Sample emission was passed through a single grating monochromator (Jobin Yvon H-10), and detected with a microchannel plate photomultiplier tube (Eldy, EM1-132).

#### Single Molecule Studies

Samples for single molecule analysis were prepared by spin-casting (60 s at 2000 rpm) dilute solutions (~10<sup>-10</sup> M) of **1** or **2** in toluene containing ~10 mg mL<sup>-1</sup> of poly(methyl methacrylate) onto thoroughly cleaned glass coverslips. Film thicknesses were checked by depth profiling (Veeco Dektak) and were found to be ~80–100 nm. Single molecules were excited by 543 nm light at 4 MHz, 1–2 ps FWHM, provided by an OPO (Spectra Physics) pumped by a regeneratively amplified Ti:sapphire laser (Spectra Physics). The light was directed into an inverted microscope (Olympus IX70) and focused at the sample through a 1.4 N.A. oil-immersion objective (Zeiss 100x). Fluorescence was collected through the same objective, split 50:50 and directed onto an avalanche photodiode (Perkin-Elmer) and through a spectrograph (Acton 150i) onto a liquid N<sub>2</sub> cooled CCD camera (Princeton). Details of the SM detection arrangement are published elsewhere.<sup>[27]</sup>

## Acknowledgements

This project is supported by Australian Research Council Discovery Project DP0664163. TDMB gratefully acknowledges The University of Melbourne Faculty of Science for the award of a Centenary Research Fellowship. We would like to thank the CRC Smartprint for financial assistance in the form of a Scholarship to CHJ. The authors also thank Dr. Scott Watkins for the depth profile measurements on polymer film samples, Dr. Michel Sliwa for technical assistance with the single molecule measurements and we acknowledge the contributions of Matthew Belousoff and Dr. Craig Forsyth in their help in obtaining crystallographic data.

- [1] P. Tinnefeld, M. Sauer, *Angew. Chem.* **2005**, *117*, 2698–2728; *Angew. Chem. Int. Ed.* **2005**, *44*, 2642–2671.
- [2] W. E. Moerner, *J. Phys. Chem. B* **2002**, *106*, 910–927.
- [3] F. Kulzer, M. Orrit, *Annu. Rev. Phys. Chem.* **2004**, *55*, 585–611.
- [4] A. C. Grimsdale, T. Vosch, M. Lor, M. Cotlet, S. Habuchi, J. Hofkens, F. C. De Schryver, K. Müllen, *J. Lumin.* **2005**, *111*, 239–253.
- [5] F. C. De Schryver, T. Vosch, M. Cotlet, M. Van der Auweraer, K. Müllen, J. Hofkens, *Acc. Chem. Res.* **2005**, *38*, 514–522.
- [6] G. Andric, J. F. Boas, A. M. Bond, G. D. Fallon, K. P. Ghiggino, C. F. Hogan, J. A. Hutchison, M. A. P. Lee, S. J. Langford, J. R. Pilbrow, G. J. Troup, C. P. Woodward, *Aust. J. Chem.* **2004**, *57*, 1011–1019.
- [7] M. Cotlet, T. Vosch, S. Habuchi, T. Weil, K. Müllen, J. Hofkens, F. De Schryver, *J. Am. Chem. Soc.* **2005**, *127*, 9760–9768.
- [8] F. Würthner, S. Ahmed, C. Thalacker and T. Debaerdemaeker, *Chem. Eur. J.* **2002**, *8*, 4742–4750.
- [9] C. Thalacker, C. Röger, F. Würthner, *J. Org. Chem.* **2006**, *71*, 8098–8105.
- [10] C. Thalacker, A. Miura, S. De Feyter, F. C. De Schryver, F. Würthner, *Org. Biomol. Chem.* **2005**, *3*, 414–422.
- [11] C. Röger, S. Ahmed, F. Würthner, *Synthesis* **2007**, 1872–1876.
- [12] C. Röger, S. Ahmed, F. Würthner, *J. Org. Chem.* **2007**, *72*, 8070–8075.
- [13] S. V. Bhosale, C. H. Jani, S. J. Langford, *Chem. Soc. Rev.* **2008**, *37*, 331–342.
- [14] H. Vollmann, H. Becker, M. Corell, H. Streeck, *Liebigs Ann. Chem.* **1937**, *531*, 1–159.
- [15] S. Bhosale, A. L. Sisson, P. Talukdar, A. Fürstenberg, N. Banerji, E. Vauthey, G. Bollot, J. Mareda, C. Röger, F. Würthner, N. Sakai, S. Matile, *Science* **2006**, *313*, 84–86.
- [16] C. Röger, M. G. Muller, M. Lysetska, Y. Miloslavina, A. R. Holzwarth, F. Würthner, *J. Am. Chem. Soc.* **2006**, *128*, 6542.
- [17] B. A. Jones, A. Facchetti, T. J. Marks, M. R. Wasielewski, *Chem. Mater.* **2007**, *19*, 2703–2705.
- [18] P. Jacquignon, N. P. Buu-Hoi, M. Mangane, *Bull. Soc. Chim. Fr.* **1964**, *10*, 2517–2523.
- [19] F. Chaignon, M. Falkenström, S. Karlsson, E. Blart, F. Odobel, L. Hammarstrom, *Chem. Commun.* **2007**, 64–66.
- [20] Two regioisomers are likely from the dibromination, those placed antipodally that is, 2,6-positions and the 2,7-dibromo NDA regioisomer. In our work, as with others, we only see evidence for the 2,6-dibromo isomer by NMR spectroscopy. If the other isomer forms in >5% yield, it is indistinguishable by both chromatographic and NMR spectroscopic techniques. The result can be explained in terms of buttressing restraints, but we cannot discount the formation of the other regioisomer conclusively.
- [21] The low solubility of this compound and lack of protons within its structure ( $\text{C}_{14}\text{O}_6\text{Br}_4$ ) makes it difficult to characterize the product by traditional means. However, mass spectrometry gave data consistent with **5**, in particular the diagnostic isotopic pattern expected for addition of four bromine atoms to the starting anhydride.
- [22] Crystal data for **5**: M.p.: > 350°C;  $\text{C}_{14}\text{Br}_4\text{O}_6$ :  $M$  = 579.64, Colorless rectangular prisms,  $0.21 \times 0.14 \times 0.13 \text{ mm}^3$ , triclinic, space group  $P-1$ ,  $a = 6.4747(13)$ ,  $b = 7.5706(15)$ ,  $c = 12.434(3) \text{ Å}$ ,  $\alpha = 91.28(3)$ ,  $\beta = 103.27(3)$ ,  $\gamma = 114.24(3)^\circ$ ,  $V = 536.22(26) \text{ Å}^3$ ,  $Z = 1$ ,  $\rho_{\text{calc}} = 2.292 \text{ g cm}^{-3}$ ,  $F_{000} = 356$ ,  $\text{MoK}_\alpha$  radiation  $\lambda = 0.71073 \text{ Å}$ ,  $T = 173(2) \text{ K}$ ,  $2\theta_{\text{max}} = 56.1^\circ$ , 9652 reflections collected, 2554 unique ( $R_{\text{int}} = 0.0501$ ).

- Final  $GoF=1.031$ ,  $RI=0.0276$ ,  $wR2=0.0602$ ,  $R$  indices based on 2240 reflections with  $I>2\sigma(I)$  (refinement on  $F^2$ ), 147 parameters, 0 restraints. Lp and absorption corrections applied,  $\mu=7.747\text{ mm}^{-1}$ .
- [23] G. D. Fallon, M. A. P. Lee, S. J. Langford, *Acta Crystallogr. E* **2003**, 59, o328–o329.
- [24] G. D. Fallon, M. A. P. Lee, S. J. Langford, P. J. Nichols, *Org. Lett.* **2004**, 6, 655–658.
- [25] The average error in these values is  $0.04\text{ \AA}$ .
- [26] T. D. M. Bell, K. P. Ghiggino, K. A. Jolliffe, M. G. Ranasinghe, S. J. Langford, M. J. Shephard and M. N. Paddon-Row, *J. Phys. Chem. A* **2002**, 106, 10079–10088.
- [27] T. Vosch, M. Cotlet, J. Hofkens, K. Van Biest, M. Lor, K. Weston, P. Tinnefeld, M. Sauer, L. Latterini, K. Müllen, F. C. De Schryver, *J. Phys. Chem. A* **2003**, 107, 6920–6931.

Received: June 22, 2009

Published online: September 16, 2009